THE JOURNAL OF PHYSICAL CHEMISTRY Letters

pubs.acs.org/JPCL

Substrate Hybridization and Rippling of Graphene Evidenced by Near-Edge X-ray Absorption Fine Structure Spectroscopy

Vincent Lee,[†] Chanro Park,[‡] Cherno Jaye,[§] Daniel A. Fischer,*[,§] Qingkai Yu,[∥,⊥] Wei Wu,[∥,⊥] Zhihong Liu,[⊥] Jiming Bao,[⊥] Shin-Shem Pei,[∥,⊥] Casey Smith,[‡] Patrick Lysaght,*[,‡] and Sarbajit Banerjee*[,†]

[†]Department of Chemistry, University at Buffalo, State University of New York, Buffalo, New York 14260-3000, [‡]Front-End Process Division, SEMATECH, 2706 Montopolis Drive, Austin, Texas 78741, [§]Materials Science and Engineering Laboratory, National Institute of Standards and Technology, Gaithersburg, Maryland 20899, [∥]Center for Advanced Materials, University of Houston, Texas 77204, and [⊥]Department of Electrical and Computer Engineering, University of Houston, Houston, Texas 77204

ABSTRACT Interfacial interactions at graphene/metal and graphene/dielectric interfaces are likely to profoundly influence the electronic structure of graphene. We present here the first angle-resolved near-edge X-ray absorption fine structure (NEXAFS) spectroscopy study of single- and bilayered graphene grown by chemical vapor deposition on Cu and Ni substrates. The spectra indicate the presence of new electronic states in the conduction band derived from hybridization of the C−π network with Cu and Ni d-orbitals. In conjunction with Raman data demonstrating charge transfer, the NEXAFS data illustrate that the uniquely accessible interfaces of two-dimensional graphene are significantly perturbed by surface coatings and the underlying substrate. NEXAFS data have also been acquired after transfer of graphene onto SiO_2/Si substrates and indicate that substantial surface corrugation and misalignment of graphene is induced during the transfer process. The rippling and corrugation of graphene, studied here by NEXAFS spectroscopy, is thought to deleteriously impact electrical transport in graphene.

SECTION Surfaces, Interfaces, Catalysis

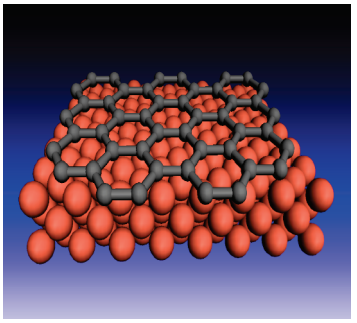

Graphene, a one-atom-thick, two-dimensional (2D) electronic system exhibiting a cornucopia of quantum transport phenomena, is constituted from a single layer of carbon atoms tightly packed within a honeycomb lattice.[1−3] Recent advances in the wafer-scale fabrication of graphene by chemical vapor deposition (CVD) methods inspire confidence that it may be possible to harness the remarkable electronic structure of graphene for applications in microelectronics and quantum logic devices.[4−7] In particular, the massive room-temperature mobilities of charge carriers in graphene[8,9] portends the possible use of this material in ultrahigh frequency transistors with an operational regime extending to the terahertz range.[2] The large phase coherence length and room-temperature ballistic conduction observed across micrometer-scale dimensions further tantalizes with possibilities for applications in spin-logic architectures.[10,11]

Much of the novel transport phenomena observed for graphene is derived from its unique electronic structure wherein electrons propagating through the honeycomb lattice behave as massless and chiral Dirac fermions, and the valence and conduction bands touch at conical Dirac points with a remarkable linear energy dispersion within ±1 eV of the Fermi energy.[3]

As graphene transitions from being merely an object of academic curiosity to real device applications, there is considerable interest regarding modifications of the characteristic graphene electronic spectrum when graphene is interfaced with other materials including metals and dielectrics.[12−14] There is a growing body of evidence that the strong bonding of graphene layers to substrates during epitaxial or CVD growth significantly alters the electronic structure of graphene.[14−16] A dead "buffer" interfacial layer exhibiting strong substrate hybridization has been reported upon the epitaxial growth of graphene on SiC and Ru substrates with only the subsequent electronically decoupled second layer exhibiting properties analogous to single-layered graphene (SLG).[14,15] We present here a systematic angle-resolved near-edge X-ray absorption fine structure (NEXAFS) spectroscopy study of graphene layers grown by CVD on Cu and Ni substrates and transferred subsequently onto SiO_2/Si substrates.

Received Date: February 15, 2010
Accepted Date: March 23, 2010
Published on Web Date: March 29, 2010

DOI: 10.1021/jz100209h | *J. Phys. Chem. Lett.* **2010**, *1*, 1247–1253

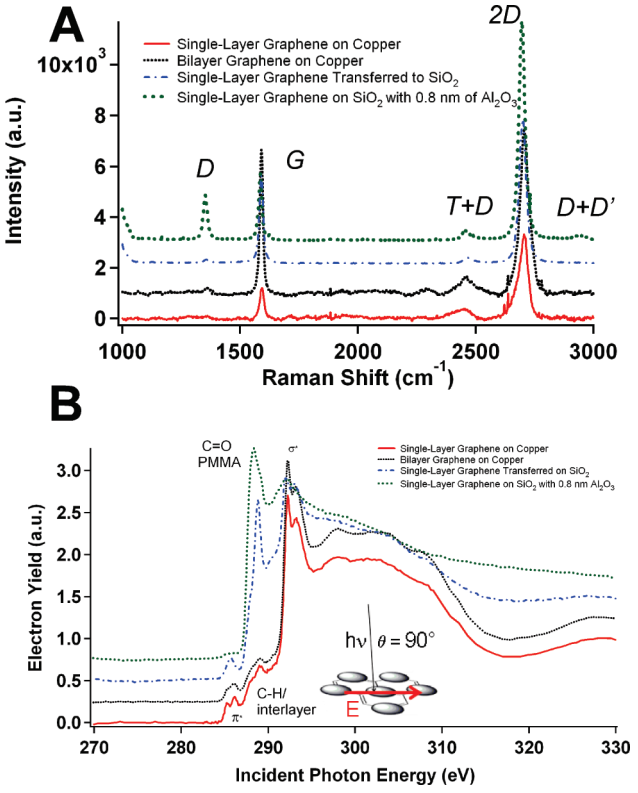

Figure 1. (A) Raman spectra acquired using 514.5 nm laser excitation for four samples: SLG on Cu, BLG graphene on Cu, SLG on Cu after transfer to a SiO_2/Si substrate, and SLG on Cu after transfer to a SiO_2/Si substrate and sputtering of a 0.8 nm Al_2O_3 dielectric layer. (B) C K-edge NEXAFS data acquired for the same four samples at normal incidence of the X-ray beam. Peak assignments of the major peaks are noted in the figure. The inset shows the relative orientation of the incident X-ray beam and its electric field vector with respect to the graphene surface.

Figure 1A shows Raman data acquired using 514.5 nm laser excitation for four graphene samples: SLG on Cu, bilayered graphene (BLG) on Cu, SLG transferred onto a SiO_2/Si substrate, and SLG on SiO_2/Si with a sputtered 0.8 nm Al_2O_3 dielectric layer. Raman spectroscopy is a powerful probe of both phonon dispersion and electron−phonon coupling, and indeed serves as a sensitive probe of both the number of graphene layers as well as the extent of the chemical/electrical doping of graphene.[17−20] Raman spectra of graphene (and graphite) are characterized by a 2-fold-degenerate in-plane E_{2g} phonon mode at the zone center, denoted as the *G*-band, observed at ∼1580 cm^{-1} and an energy-dispersive 2*D* (or *G*′) mode at ∼2700 cm^{-1} arising from a double resonance process involving the scattering of two phonons with opposite moments adjacent to the **K** point of the graphene Brillouin zone (BZ).[19] A characteristic feature of SLG is that the double-resonance 2*D* band is much stronger in intensity than the E_{2g} *G*-band.[18] This enhanced intensity of the 2*D* mode is clearly noted for the purported SLG sample on Cu (Figure 1A). Further verification of the single-layered nature of the sample comes from the line shape of the 2*D* band;[19] the 2*D* band for SLG can be fitted with a single Lorentzian, although the full width at half-maximum (fwhm) is appreciably broader than reported for micromechanically cleaved graphene.[17,20] The predominantly BLG sample shows slightly greater asymmetry of the 2*D* band. Notably, the *G*-bands for both SLG and BLG graphene are shifted to higher frequencies and are also significantly broadened relative to undoped micromechanically cleaved graphene.[17,20] The origin of these spectral changes is likely the doping of graphene due to interactions with the underlying Cu substrate. Specifically, for metals, phonons are somewhat screened by electronic states at certain points of the BZ, as dictated by the shape of the Fermi surface. This gives rise to the Kohn anomaly, which softens the graphene modes, especially the E_{2g} mode.[19,20] Upon chemical doping, the Fermi surface is altered, and the Kohn anomaly departs from $q = 0$ because of the change in carrier concentration, resulting in stiffening of the *G*-mode to higher frequencies, as is clearly noted for the graphene samples on Cu in Figure 1A.[19,20] Significantly, doping also induces a decrease in the $I(2D)/I(G)$ ratios.[15,19] The observed frequencies, lineshapes, and intensity ratios are thus indicative of charge transfer between the graphene layers and the underlying Cu substrate. Other factors such as temperature, stress, pressure, and deformation can also give rise to pronounced shifts in the Raman spectral features of graphene. The Raman spectroscopy results are consistent with recent density functional theory (DFT) predictions that the adsorption of Cu onto graphene substantially preserves the intrinsic graphene electronic structure but shifts the Fermi level.[12] Notably, upon transfer to SiO_2/Si, the *G*-band shifts from ∼1592 to 1590 cm^{-1} and subsequently to ∼1586 cm^{-1} after coating with the dielectric. The fwhm of the peak is also narrowed by ∼3.0 cm^{-1} upon transfer to SiO_2/Si and deposition of the dielectric layer likely due to changes in the extent of doping. Residual metal ions from the etching process along with contamination from poly(methyl methacrylate) (PMMA) could account for the persistence of some doping even upon transfer. Dielectric deposition also likely induces appreciable stress that could be responsible for altering the lineshapes and peak positions of the transferred graphene samples coated with 0.8 nm Al_2O_3.

Notably, the intensity of the weak *D*-band is not significantly altered upon transfer, suggesting that the transfer process does not significantly increase the defect density or cause fragmentation of graphene domains. However, upon deposition of the Al_2O_3 gate dielectric layer, a sharp increase in the intensity of the *D*-band is noted. Since this spectral feature originates from a double-resonant intravalley process involving electron scattering at a defect site,[19] the activation of this mode suggests that the deposition of Al_2O_3 induces symmetry breaking of graphene with the probable incorporation of defect sites.[13] A new feature also appears at ∼2930 cm^{-1} and can be attributed to a combination $D+D'$ mode, which is also activated by scattering at defect sites.

Misalignment and alterations to the graphene electronic spectrum due to interfacial phenomena have been further probed by carbon K-edge NEXAFS spectroscopy. NEXAFS spectroscopy involves the use of low-energy X-rays to promote electrons from core levels to partially filled and unoccupied states and is thus a powerful local probe of the electronic structure above the Fermi level.[21−23] The peak positions and lineshapes of the observed NEXAFS resonances represent, to

DOI: 10.1021/jz100209h | J. Phys. Chem. Lett. 2010, 1, 1247–1253

first approximation, a distorted replica of the unoccupied density of states (UDOS). The dipole selection rules operational for NEXAFS (change in the angular momentum quantum number, $\Delta l = \pm 1$; change in spin disallowed) enable frontier orbital states to be examined depending on their symmetry by varying the incident angle of the linearly polarized synchrotron X-ray beam.[24]

Figure 1B shows NEXAFS data acquired for the same four graphene samples studied by Raman spectroscopy. The spectra have been acquired at 85° incidence of the X-ray beam (θ represents the angle between the incident beam and the substrate surface, inset to Figure 1B) and are presented after pre- and post-edge normalization. The acquired partial-electron-yield signals, acquired with an energy resolution of ~0.1 eV, have been normalized by the incident beam intensity obtained from the photoemission yield of a Au grid with 90% transmittance located along the beam path. A carbon mesh (with a C=C π^* resonance at 285.1 eV), also located along the beam path, is used for energy calibration. The lowest-energy feature in Figure 1B is the peak (envelope of peaks) centered at ca. 285.5−285.9 eV, corresponding to transitions from C1*s* core levels to graphene conduction band π^* states in the vicinity of the *M* and *L* points of the BZ.[24−27] The most prominent features in the spectra presented in Figure 1B are the resonances at ~292.2 eV corresponding to transitions to dispersionless σ^* states at the **Γ**-point of the graphene BZ.[24,26,27] At normal incidence of the polarized X-ray beam ($\theta = 90°$, as per Figure 1B, inset), the electric-field vector **E** lies within the graphene plane, and thus transitions to states of σ symmetry are enhanced, accounting for the strong intensity of these features in Figure 1B.

The normal incidence spectrum for the SLG sample on Cu indicates the curious splitting of the π^* peak into two distinct resonances centered at ~285.3 and 286.1 eV. Interestingly, this peak splitting with the appearance of the distinctive low-energy feature is visible but less pronounced for BLG on Cu and completely disappears upon transfer to the SiO_2/Si substrate (Figure 1B, inset). The said low-energy feature is most pronounced at normal incidence when the contribution from the π^* peak is at its minimum, but is also discernible at other polarization angles and indeed even at glancing incidence at least two Voight functions including a low-energy component are required to accurately fit the envelope of π^* peaks. We attribute this resonance to states arising from the hybridization of graphene with the underlying Cu substrate. Consistent with this assignment, this spectral feature is attenuated in BLG since the second layer is likely to be electronically decoupled from the Cu substrate to a greater extent. Furthermore, upon transfer to the SiO_2/Si substrate, the low-energy feature completely disappears (since there is no significant hybridization of amorphous SiO_2 with graphene π states).[15] Indeed, it is not surprising that a new electronic state appears in the conduction band from the hybridization of out-of-plane graphene C2p_z orbitals, which have the correct symmetry for overlap with Cu d-orbitals. In this context, the strong hybridization of graphene with underlying SiC and Ru substrates have been reported,[10,14,15] and for the former substrate, photoemission measurements indicate that covalent bonding of the first graphene layer with the SiC substrate completely disrupts the delocalized hexagonal π-electron network but retains the σ network with sp^2 hybridization.[14] Unlike epitaxial samples with strongly bound buffer layers, the substrate−graphene separation for CVD-grown samples on Cu is expected to be much larger (predicted to be ~3.3 Å),[12] and indeed the Raman data and facile transfer onto other substrates indicates relatively weaker covalent bonding of graphene to the Cu substrate. The assignment of the low-energy component of the π^* peak to substrate hybridization is further corroborated by Figure S1 in the Supporting Information, which shows the C K-edge NEXAFS spectrum of graphene grown by CVD on Ni substrates.[4] The low-energy split-off feature attributed to hybridization of C2p_z with Ni d-orbitals is more pronounced in intensity than in the Cu case, likely because of stronger substrate hybridization. Indeed, theoretical predictions suggest an equilibrium separation of only 2.05 Å for graphene on Ni (as compared to ~3.3 Å for graphene on Cu).[12] Substrate hybridization is clearly less pronounced on Cu and Ni as compared to Ru and SiC (note that equilibrium separations have been measured to be on the order of 1.45 Å for Ru and 1.65 Å for 4H-SiC(0001)),[15] and, consequently, the π network is still preserved, and, despite appreciable covalent bonding, the graphene layers can be transferred to other substrates and show distinctive Raman spectra; consequently, SLG grown by CVD onto Cu and Ni substrates do not show the dead "buffer" layers observed on Ru and SiC. In other words, there appears to be a continuum of covalent interactions for graphene on different substrates that is reflected in the C K-edge NEXAFS spectra; the degree of substrate hybridization (extent of covalent bonding), reflecting perturbation of the graphene π-network, is smaller (but still appreciable) for CVD-grown graphene on Cu and Ni as compared to expitaxial graphene on Ru and SiC, which is further consistent with the measured and predicted equilibrium separation distances.

Some DFT predictions of interfacial interactions of graphene with metal surfaces and adsorbed metal adatoms also generally validate the above assignment.[12,16,28] For example, a down-shift of the π-band by ~0.5 eV in energy in majority spin and ~1.5 eV in minority spin is predicted upon the hybridization of d-orbitals of Co adatoms with C2p_z orbitals of graphene.[28] Hybertsen and co-workers also predicted significant electronic coupling between the graphene π-network and an underlying Co surface that depends strongly on the registry of the two materials.[16] These authors note strong interactions at the **K**-point between d_{z2} states on the Co surface and 2p_z orbitals on carbon atoms situated directly above Co sites.

Features beyond 296 eV in the spectra in Figure 1B arise from transitions to states of mostly σ symmetry[27] and are seen to be more pronounced for BLG. This is consistent with a multiple-scattering view of NEXAFS wherein the molecular cage of surrounding C atoms for an absorbing atom in SLG is smaller than in BLG.[25] For the SLG samples transferred onto SiO_2, a prominent resonance attributable to −C=O moieties appears at ~288.6 eV between the π^* and σ^* resonances, originating from residual PMMA from the transfer process. Notably, remnant PMMA and Fe impurities are detected irrespective of the resist stripping process (the latter in Fe *L*

DOI: 10.1021/jz100209h | J. Phys. Chem. Lett. 2010, 1, 1247–1253

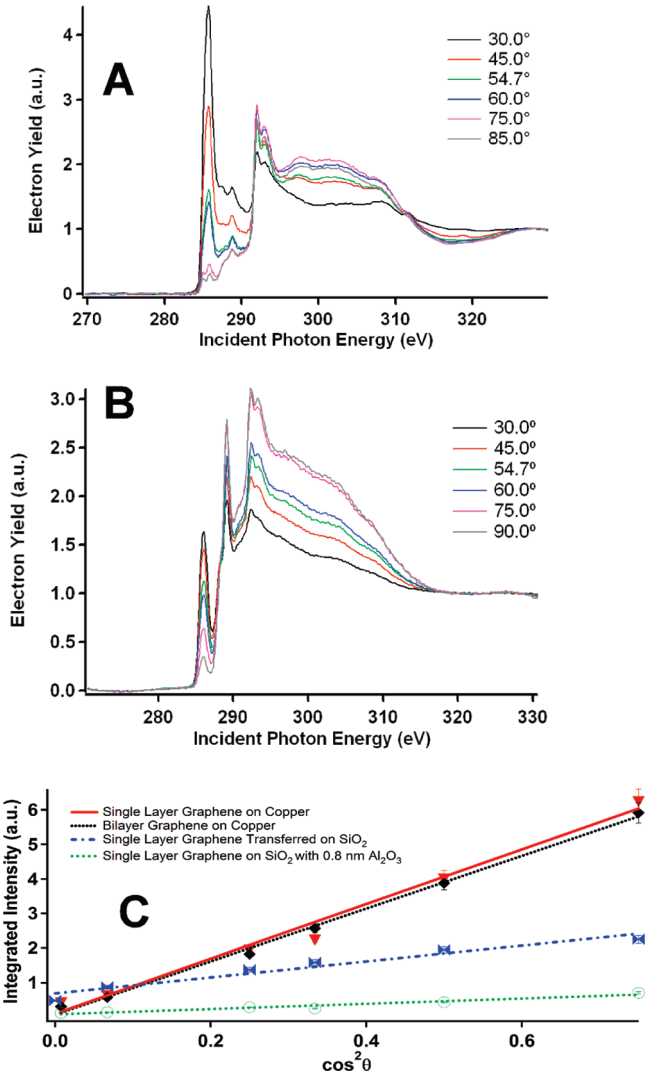

Figure 2. (A) Angle-resolved C K-edge NEXAFS spectra measured for SLG on Cu. (B) Angle-resolved C K-edge NEXAFS spectra measured for the SLG after transfer to SiO_2/Si. (C) Integrated intensity of the π^* resonance versus the incident angle for four samples: SLG on Cu, BLG graphene on Cu, SLG on Cu after transfer to a SiO_2/Si substrate, and SLG on Cu after transfer to a SiO_2/Si substrate and sputtering of a 0.8 nm Al_2O_3 dielectric layer.

NEXAFS spectra). Upon deposition of the dielectric, some diminution of the graphene π^* features is observed, likely as a result of the dilution of the graphene contribution to the spectrum by surface carbon contamination.

Nevertheless, for SLG on Cu without any chemical treatment, two distinct peaks are discernible at ~287.6 and ~289.0 eV between the π^* and σ^* resonances. The assignment of these intermediate peaks has been a topic of enduring contention over the past several decades.[25,26,29] In particular, controversy still swirls regarding the assignment of a peak in the 288−289 eV range ascribed by some to be the signature of a dispersionless interlayer state within the low-symmetry region of the graphite BZ;[25,26] others have vigorously contested this assignment and have proposed alternately that this feature arises from residual −COOH moieties present even in pristine graphite.[29,30] Given the strongly reducing conditions and high temperatures (1000 °C) operational for graphene synthesis by CVD, the presence of a sufficient density of carboxylic-acid moieties on the graphene surface to give rise to a spectral feature of the observed magnitude is quite unlikely. The relative constancy of the intensity of this feature above the edge jump noted upon varying the incident angle (Figure 2A) also suggests transitions to a state that has neither σ nor π symmetry. Consequently, we ascribe this distinctive ~289.0 eV feature to the interlayer state of SLG with charge density residing primarily above and below the graphene basal plane. This feature has been predicted to occur ~4−7.5 eV above the Fermi level, and a recent theoretical study by Silkin and coworkers ascribes its origin to intersheet hybridization with the first even-numbered member of a series of image-potential states.[31] Consistent with their prediction that the interaction of graphene with a substrate will shift the interlayer state to slightly higher energies, we note that our interlayer peak appears to be shifted to higher energy by ~1.0 eV from observations of Pacile for suspended graphene.[25] Note that a simple resolution to the longstanding interlayer controversy can be based on the predication that NEXAFS resonances for interlayer states are serendipitously closely overlapped with the spectral signatures of −C═O moieties. Consistent with the assignment noted above, Figure S2 in the Supporting Information shows C K-edge NEXAFS spectra acquired for graphene samples on Cu at magic angle incidence after annealing at temperatures up to 700 °C. No diminution of the peak ascribed to the interlayer state is observed, further corroborating that this feature does not arise from surface functional groups or adsorbed species.[25b] This leaves the 287.6 eV shoulder observed in NEXAFS spectra of SLG on Cu as the sole feature requiring assignment. Given the strongly reducing conditions used for graphene synthesis by CVD, it would not be surprising if edge sites of graphene domains were passivated with C−H bonds. Indeed, C−H σ^* states for amorphous carbon films have been noted at 287.5 eV.[22]

Figure 2A shows angle-resolved C K-edge NEXAFS spectra acquired for the SLG sample grown on Cu before and after transfer to the SiO_2/Si substrate. In the case of graphene, when the electric-field vector **E** lies along the basal plane, transitions to frontier orbital states of σ symmetry are enhanced, whereas when **E** is perpendicular to the graphene basal plane, transitions to the out-of-plane π-network constituted from C2p_z orbitals are increased in intensity (Figure 1B, inset).[24] This strong orientation dependence of transition probabilities thus makes NEXAFS a sensitive probe of the alignment and orientation of molecular monolayers, layered materials, and thin films.[21,23,24,27,32,33]

The π^* resonance of the SLG sample shown in Figure 2A clearly shows very extensive dichroism. The intensity of the π^* peak monotonically decreases with increasing angle of incidence as the projection of **E** onto the basal planes progressively increases. Analogous albeit less pronounced dichroism is also observed for the SLG sample after transfer to SiO_2/Si (Figure 2B). The latter set of spectra also show pronounced C−O σ^* and C═O π^* resonances arising from

DOI: 10.1021/jz100209h | J. Phys. Chem. Lett. 2010, 1, 1247–1253

Table 1. DRs Indicating Extent of Corrugation and Misalignment for Four Samples: SLG on Cu, BLG on Cu, SLG on Cu after Transfer to a SiO_2/Si Substrate, and SLG on Cu after Transfer to a SiO_2/Si Substrate and Sputtering of a 0.8 nm Al_2O_3 Dielectric Layer[a]

sample	DR
SLG on Cu*	$-0.97 \pm {}^{0.08}_{0.03}$
BLG on Cu*	$-0.98 \pm {}^{0.08}_{0.02}$
SLG transferred to SiO_2/Si	-0.72 ± 0.06
SLG transferred onto SiO_2/Si with a 0.8 nm Al_2O_3 layer	-0.80 ± 0.06

[a] Note that the maximum possible value of |DR| is 1.

PMMA residues. Figure 2C depicts a plot of the integrated π^* intensities versus the incident angles.

As a quantitative measure of the extent of alignment or corrugation, it is useful to define a dichroic ratio (DR):[24,34]

$$\mathrm{DR} = \frac{(I_\perp - I_\parallel)}{(I_\perp + I_\parallel)} \quad (1)$$

where $I_\perp$ and $I_\parallel$ are the extrapolates at $\theta = 90°$ and $\theta = 0°$, respectively, of the integrated intensity of the π^* resonance. The extrapolation procedure may lead to a slight error in deducing the DR value reflected in the error bars. A DR value of 0 is expected for a sample with completely random alignment of π-orbitals (such as a randomly coiled amorphous polymer), and a DR value of -1 is expected for a perfectly flat sample. Table 1 indicates the DR values determined for the samples measured in this study. As a comparison, a DR value of approximately -0.90 was measured for highly ordered pyrolitic graphite (HOPG),[33] whereas in previous studies of chemically derived graphene within electrophoretically deposited films, we have measured DR values ranging from -0.47 to -0.59.[23,24] Clearly, the *DR* values measured here for the SLG and BLG graphene samples are remarkably high (nearly -1), indicating the excellent local alignment and crystallinity of the graphene domains. The atomic force microscopy (AFM) images in Figure S3 of the Supporting Information show that Cu foils present a rather smooth surface (root-mean-square (rms) roughness of 0.17 nm), which is likely a prerequisite for obtaining such high DR values. Note that (azimuthal) angle-resolved measurements have not been performed in the basal plane since individual graphene domains on Cu are not expected to be oriented with respect to one another. Based on Raman mapping and transmission electron microscopy (TEM) images, very large domains are known to be produced by the CVD process,[7] and, consequently, the contributions from edge sites will be minimal. The transfer process clearly introduces significant corrugation/rippling and misalignment, likely because graphene on soft PMMA (after etching away of the Cu substrate) may be able to deform essentially as a flexible membrane.[2,3] While SLG and BLG graphene samples on Cu show uniformly high DR values, considerable variability is observed from sample to sample upon transfer to SiO_2/Si, which is not surprising given the variables involved in the transfer process. The highest DR value obtained for transferred graphene on SiO_2/Si is ~0.72, which still indicates substantial in-plane alignment but is significantly lower than the values observed on Cu. The AFM images and rms roughness values deduced for SiO_2/Si substrates (Figure S3, Supporting Information) do not show appreciably increased roughness, suggesting that the lower DR ratios observed after transfer are a consequence of the poor fidelity of the transfer process rather than a reflection of substrate roughness. The increased corrugation and rippling of graphene have serious implications for the mobilities of charge carriers since electrons propagating through graphene are thought to be scattered by corrugations in the graphene sheet through a potential approximately proportional to the square of the local curvature.[3,35]

In conclusion, we present the first NEXAFS measurements of SLG and BLG supported on metal substrates and observe clear evidence of substrate hybridization between C2p_z orbitals and d-orbitals on Cu and Ni. A distinctive interlayer feature is also observed for the as-grown sample and is attributed to states originating from intersheet hybridization with the lowest energy members of image potential states. Systematic angle-resolved measurements of CVD-grown graphene before and after transfer onto a SiO_2/Si substrate evidence the induction of increased rippling and corrugation during the transfer process.

EXPERIMENTAL METHODS

Graphene was grown on Cu foils by a CVD process using a CH_4/H_2/Ar mixture as the feed gas under ambient pressure.[6,7] Samples that are predominantly SLG or BLG were obtained by varying the concentration of CH_4.[5,7] The domain sizes for SLG exceed several micrometers, as indicated by Raman mapping and TEM experiments.[7] Apart from the Raman data presented in Figure 1A, evidence for the single- and bilayered nature of graphene is derived from electrical transport measurements, clearly demonstrating the ambipolar field effect (with on/off ratio ~5 and carrier mobilities up to ~3000 $cm^2/(V\,s)$) and the characteristic "half-integer" quantum Hall effect for graphene samples transferred onto insulating substrates.[7] Subsequent to graphene growth, a layer of PMMA was spun onto the SLG sample, and the Cu interface was etched using an aqueous solution of $Fe(NO_3)_3$.[7] The released graphene was then stamped onto a SiO_2(300 nm)/Si substrate. A gate dielectric layer was deposited by sputtering 0.8 nm Al and allowing it to oxidize in air to Al_2O_3.

Carbon K-edge NEXAFS data were acquired at NIST beamline U7A of the National Synchrotron Light Source at Brookhaven National Laboratory. A toroidal spherical grating monochromator with 600 lines/mm was used to acquire the C K-edge data. The slits were set at 30 μm × 30 μm. The spectra were acquired in partial electron yield (PEY) mode with a channeltron electron multiplier detector with a -150 V entrance grid bias to enhance surface sensitivity. A charge-compensating electron charge gun was used to eliminate the effects of charging.

SUPPORTING INFORMATION AVAILABLE C K-edge data acquired at normal incidence for SLG grown on a nickel substrate and for few-layered graphene on Cu after annealing at temperatures up to 700°C as well as AFM images of SiO_2/Si and Cu foil showing the very minimal surface roughness values measured for the two substrates. This material is available free of charge via the Internet at http://pubs.acs.org

DOI: 10.1021/jz100209h | *J. Phys. Chem. Lett.* **2010**, *1*, 1247–1253

AUTHOR INFORMATION

Corresponding Author:

*To whom correspondence should be addressed. E-mail: dfischer@nist.gov (D.A.F.); Pat.Lysaght@sematech.org (P.L.); sb244@buffalo.edu (S.B.).

ACKNOWLEDGMENT This work was primarily supported by the NSF under DMR0847169. S.B. acknowledges the NSLS for travel funding through the FSRSP Program. Certain commercial names are presented in this manuscript for purposes of illustration and do not constitute an endorsement by NIST.

REFERENCES

(1) Geim, A. K.; Novoselov, K. S. The Rise of Graphene. *Nat. Mater.* **2007,** *6*, 183–191.

(2) Geim, A. K. Graphene: Status and Prospects. *Science* **2009,** *324*, 1530–1534.

(3) Castro Neto, A. H.; Guinea, F.; Peres, N. M. R.; Novoselov, K. S.; Geim, A. K. The Electronic Properties of Graphene. *Rev. Mod. Phys.* **2009,** *81*, 109–162.

(4) Kim, K. S.; Zhao, Y.; Jang, H.; Lee, S. Y.; Kim, J. M.; Kim, K. S.; Ahn, J.-H.; Kim, P.; Choi, J.-Y.; Hong, B. H. Large-Scale Pattern Growth of Graphene Films for Stretchable Transparent Electrodes. *Nature* **2009,** *457*, 706–710.

(5) Lee, Y.; Bae, S.; Jang, H.; Jang, S.; Zhu, S.-E.; Sim, S. H.; Song, Y. I.; Hong, B. H.; Ahn, J.-H. Wafer-Scale Synthesis and Transfer of Raphene Films. *Nano Lett.* **2010,** *10*, 490–493.

(6) Li, X.; Cai, W.; An, J.; Kim, S.; Nah, J.; Yang, D.; Piner, R.; Velamakanni, A.; Jung, I.; Tutuc, E.; Banerjee, S. K.; Colombo, L.; Ruoff, R. S. Large-Area Synthesis of High-Quality and Uniform Graphene Films on Copper Foils. *Science* **2009,** *324*, 1312–1314.

(7) Cao, H.; Yu, Q.; Jauregui, L.; Tian, J.; Wu, W.; Liu, Z.; Jalilian, R.; Benjamin, D. K.; Jiang, Z.; Bao, J.; Pei, S. S. S.; Chen, Y. P. Electronic Transport in Chemical Vapor Deposited Graphene Synthesized on Cu: Quantum Hall Effect and Weak Localization. *Appl. Phys. Lett.*, in press.

(8) Bolotin, K. I.; Sikes, K. J.; Jiang, Z.; Klima, M.; Fudenberg, G.; Hone, J.; Kim, P.; Stormer, H. L. Ultrahigh Electron Mobility in Suspended Graphene. *Solid State Commun.* **2008,** *146*, 351–355.

(9) Morozov, S. V.; Novoselov, K. S.; Katsnelson, M. I.; Schedin, F.; Elias, D. C.; Jaszczak, J. A.; Geim, A. K. Giant Intrinsic Carrier Mobilities in Graphene and Its Bilayer. *Phys. Rev. Lett.* **2008,** *100*, 016602/1–4.

(10) Berger, C.; Song, Z.; Li, X.; Wu, X.; Brown, N.; Naud, C.; Mayou, D.; Li, T.; Hass, J.; Marchenkov, A. N.; Conrad, E. H.; First, P. N.; de Heer, W. A. Electronic Confinement and Coherence in Patterned Epitaxial Graphene. *Science* **2006,** *312*, 1191–1196.

(11) Tombros, N.; Jozsa, C.; Popinciuc, M.; Jonkman, H. T.; van Wees, B. J. Electronic Spin Transport and Spin Precession in Single Graphene Layers at Room Temperature. *Nature* **2007,** *448*, 571–574.

(12) Giovannetti, G.; Khomyakov, P. A.; Brocks, G.; Karpan, V. M.; van den Brink, J.; Kelly, P. J. Doping Graphene with Metal Contacts. *Phys. Rev. Lett.* **2008,** *101*, 026803/1–4.

(13) Jin, Z.; Su, Y.; Chen, J.; Liu, X.; Wu, D. Study of AlN Dielectric Film on Graphene by Raman Microscopy. *Appl. Phys. Lett.* **2009,** *95*, 233110/1–3.

(14) Kim, S.; Ihm, J.; Choi, H. J.; Son, Y.-W. Origin of Anomalous Electronic Structures of Epitaxial Graphene on Silicon Carbide. *Phys. Rev. Lett.* **2008,** *100* (17), 176802/1–4.

(15) Sutter, P. W.; Flege, J.-I.; Sutter, E. A. Epitaxial Graphene on Ruthenium. *Nat. Mater.* **2008,** *7*, 406–411.

(16) Eom, D.; Prezzi, D.; Rim, K. T.; Zhou, H.; Lefenfeld, M.; Xiao, S.; Nuckolls, C.; Hybertsen, M. S.; Heinz, T. F.; Flynn, G. W. Structure and Electronic Properties of Graphene Nanoislands on Co(0001). *Nano Lett.* **2009,** *9*, 2844–2848.

(17) Ferrari, A. C.; Meyer, J. C.; Scardaci, V.; Casiraghi, C.; Lazzeri, M.; Mauri, F.; Piscanec, S.; Jiang, D.; Novoselov, K. S.; Roth, S.; Geim, A. K. Raman Spectrum of Graphene and Graphene Layers. *Phys. Rev. Lett.* **2006,** *97*, 187401/1–4.

(18) Dresselhaus, M. S.; Dresselhaus, G.; Hoffmann, M. Raman Spectroscopy as a Probe of Graphene and Carbon Nanotubes. *Philos. Trans. R. Soc. A* **2008,** *366*, 231–236.

(19) Ferrarri, A. C. Raman Spectroscopy of Graphene and Graphite: Disorder, Electron−Phonon Coupling, Doping, and Nonadiabatic Effects. *Solid State Commun.* **2007,** *143*, 47–57.

(20) Pisana, S.; Lazzeri, M.; Casiraghi, C.; Novoselov, K. S.; Geim, A. K.; Ferrari, A. C.; Mauri, F. Breakdown of the Adiabatic Born−Oppenheimer Approximation in Graphene. *Nat. Mater.* **2007,** *6*, 198–201.

(21) Stohr, J. *NEXAFS Spectroscopy*; Springer, Berlin, 1992.

(22) Chen, J. G. NEXAFS Investigations of Transition Metal Oxides, Nitrides, Carbides, Sulfides, and Other Interstitial Compounds. *Surf. Sci. Reports* **1997,** *30*, 1–152.

(23) Hemraj-Benny, T.; Banerjee, S.; Sambasivan, S.; Balasubramanian, M.; Fischer, D. A.; Eres, G.; Puretzky, A. A.; Geohegan, D. B.; Lowndes, D. H.; Han, W.; Misewich, J. A.; Wong, S. S. Near-Edge X-ray Absorption Fine Structure Spectroscopy as a Tool for Investigating Nanomaterials. *Small* **2006,** *2*, 26–35.

(24) Lee, V.; Whittaker, L.; Jaye, C.; Baroudi, K. M.; Fischer, D. A.; Banerjee, S. Large-Area Chemically Modified Graphene Films: Electrophoretic Deposition and Characterization by Soft X-ray Absorption Spectroscopy. *Chem. Mater.* **2009,** *21*, 3905–3916.

(25) (a) Pacile, D.; Papagno, M.; Rodriguez, A. F.; Grioni, M.; Papagno, L.; Girit, C. O.; Meyer, J. C.; Begtrup, G. E.; Zettl, A. Near-Edge X-ray Absorption Fine Structure Investigation of Graphene. *Phys. Rev. Lett.* **2008,** *101*, 066806/1–4.(b) Pacile, D.; Papagno, M.; Rodriguez, A. F.; Grioni, M.; Papagno, L.; Girit, C. O.; Meyer, J. C.; Begtrup, G. E.; Zettl, A. Reply to Comment. *Phys. Rev. Lett.* 099702/1.

(26) Fischer, D. A.; Wentzcovich, R. M.; Carr, R. G.; Continenza, A.; Freeman, A. J. Graphitic Interlayer States: A Carbon *K* Near-Edge X-ray-Absorption-Fine-Structure Study. *Phys. Rev. B* **1991,** *44*, 1427–1429.

(27) Rosenberg, R. A.; Love, P. J.; Rehn, V. Polarization-Dependent C(*K*) Near-Edge X-ray-Absorption Fine Structure of Graphite. *Phys. Rev. B* **1986,** *33*, 4034–4037.

(28) Mao, Y.; Yuan, J.; Zhong, J. Density Functional Calculation of Transition Metal Adatom Adsorption on Graphene. *J. Phys.: Condens. Matter* **2008,** *20*, 115209/1–6.

(29) Jeong, H. K.; Noh, H. J.; Kim, J. Y.; Colakerol, L.; Glans, P. A.; Jin, M. H.; Smith, K. E.; Lee, Y. H. Comment on "Near-Edge X-ray Absorption Fine Structure Investigation of Graphene. *Phys. Rev. Lett.* **2009,** *102*, 099701/1.

(30) Jeong, H. K.; Noh, H. J.; Kim, J. Y.; Jin, M. H.; Park, C. Y.; Lee, Y. H. X-ray Absorption Spectroscopy of Graphite Oxide. *Europhys. Lett.* **2008,** *82*, 67004/1–5.

(31) Silkin, V. M.; Zhao, J.; Guinea, F.; Chulkov, E. V.; Echenique, P. M.; Petek, H. Image Potential States in Graphene. *Phys. Rev. B* **2009,** *80*, 121408/1–4.

(32) Velazquez, J. M.; Jaye, C.; Fischer, D. A.; Banerjee, S. Near Edge X-Ray Absorption Fine Structure Spectroscopy Studies of Single-Crystalline V_2O_5 Nanowire Arrays. *J. Phys. Chem. C* **2009,** *113*, 7639–7645.

(33) Banerjee, S.; Hemraj-Benny, T.; Sambasivan, S.; Fischer, D. A.; Misewich, J. A.; Wong, S. S. Near-Edge X-ray Absorption Fine Structure Investigations of Order in Carbon Nanotube-Based Systems. *J. Phys. Chem. B* **2005,** *109*, 8489–8495.
(34) Smith, A. P.; Ade, H. Quantitative Orientational Analysis of a Polymeric Material (Kevlar Fibers) with X-ray Microspectroscopy. *Appl. Phys. Lett.* **1996,** *69*, 3833–3835.
(35) Katsnelson, M. I.; Geim, A. K. Electron Scattering on Microscopic Corrugations in Graphene. *Philos. Trans. R. Soc. A* **2008,** *366*, 195–204.

DOI: 10.1021/jz100209h | *J. Phys. Chem. Lett.* **2010,** *1*, 1247–1253